



Cite this: DOI: 10.1039/d5cy01557j

Tuning the active phase and surface chemistry of a CO₂ hydrogenation Co/TiO₂ catalyst with UV light

D. N. Maaskant,^a P. T. Prins,^a N. S. Genz,^b
B. M. Weckhuysen^a and M. Monai^{*a}

To improve catalytic performance, it is important to control the state of the active phase of catalysts (e.g., metallic, oxidic, or carbide). However, conventional pretreatments (e.g., heating) often cause unwanted side-effects, like sintering and active phase encapsulation. Here, we propose UV light illumination as an alternative approach to tune the active phase under reaction conditions. We showcase this possibility using a Co/TiO₂ catalyst for CO₂ hydrogenation. UV light illumination resulted in an increase in the percentage of reduced Co (i.e., 93 vs. 97% metallic cobalt for dark vs. light), as revealed by X-ray absorption spectroscopy. Furthermore, using operando Fourier transform infrared spectroscopy under CO₂ hydrogenation conditions, we observed a light-induced change in surface coverage of different species, such as CO*, (bi)carbonates and formates. When switching between dark and light conditions, a reversible increase in activity was observed, accompanied by a decrease in the IR absorption bands of formates and CO*. We propose that the reduction of cobalt is due to a charge transfer mechanism from the conduction band of the titania support to the conduction band of the cobalt metal (oxide) nanoparticles. On the other hand, we attribute CO desorption to a metal-to-ligand charge transfer, from the d-band of the cobalt metal (oxide) nanoparticles to the adsorbed CO molecules. While UV light illumination is more commonly used to enhance catalytic performance, we demonstrate its application to tune the active phase of the catalyst, offering advantages over conventional methods that suffer from undesired effects, like metal (oxide) nanoparticle sintering.

Received 18th December 2025,
Accepted 2nd April 2026

DOI: 10.1039/d5cy01557j

rsc.li/catalysis

Introduction

The oxidation state of the active phase of heterogeneous catalyst materials is an important factor for their overall stability, activity and selectivity.^{1–3} Examples of catalytic reactions affected by the composition and phase of the active phase are CO and CO₂ hydrogenation, where the active phase can include carbides, oxides, and metal phases.^{2,4,5} As the active phase is of high relevance for catalytic performance, tuning of the active phase is important. Conventionally, chemical and/or heating pretreatments are used to obtain the desired active phase. For example, reduction under H₂ gas at high temperatures is used to obtain metal phases,² and flowing CO in the absence of H₂ or lean H₂ concentration over the catalyst can be used to obtain metal carbides.⁶ Furthermore, using

reducing or oxidative treatments, it is possible to induce strong-metal support interactions (SMSI), i.e. overlayer formation of the support material over metal nanoparticles.⁷ The appropriate degree of SMSI can enhance catalytic performance for CO₂ hydrogenation, while excessive SMSI can result in diminished catalytic efficiency.⁸ Hence, reductive and oxidative pretreatments are effective methods to tweak catalyst performance.

However, a disadvantage of such pretreatments is the undesired sintering of metal (oxide or carbide) nanoparticles that can be caused by elevated temperatures and pressures.⁹ Moreover, solid catalysts are dynamic and can change under reaction conditions.¹⁰ This can lead to a (partial) reversal of the pretreatment applied.⁹ While reaction conditions (e.g., temperature and pressure) can be used to tweak the active phase, they can also affect the thermodynamic equilibrium, activity and selectivity.^{11,12} Thus, a way of tuning the active phase during catalytic reactions with an external stimulus is desirable. Shetty *et al.* describe several categories of external stimuli in their review article, such as mechanical stimuli, surface acoustic waves and light.¹⁰ Specifically, light as an external stimulus is gaining increasing attention for photo-

^a Inorganic Chemistry and Catalysis, Institute for Sustainable and Circular Chemistry, Department of Chemistry, Faculty of Science, Utrecht University, Universiteitsweg 99, Utrecht, 3584 CG, The Netherlands. E-mail: m.monai@uu.nl

^b Paul Scherrer Institute, PSI Center for Energy and Environmental Sciences, Villigen PSI, CH-5232, Switzerland



assisted catalysis as it can tune performance and can be switched on and off easily for on-demand catalytic conversions.^{13–15}

Different mechanisms underlying photo-assisted catalysis are reported, *e.g.*, plasmon band excitation, photothermal effects, excitation of adsorbates and excitation of valence band electrons to the conduction band.^{13–15} It was shown that light can change the oxidation state of catalyst materials (*e.g.*, in Cu/ZnO/Al₂O₃,¹⁴ and in Au/Pd/Cu particles¹⁶). Moreover, it is possible to use UV light irradiation to induce SMSI in Pd/TiO₂, Pt/TiO₂ and Pd/ZnO catalysts.¹⁷ Though photo-assisted catalysis itself is gaining increasing attention,^{13–15} the use of light to tune the active phase is less explored.

Here, we investigate how UV irradiation during the catalytic reaction alters the active phase of a Co/TiO₂ catalyst under reaction conditions, and discuss the potential of light to serve as an additional tuning parameter beyond temperature, pressure, and gas composition. We used CO₂ hydrogenation as a model reaction because of its relevance for CO₂ utilization.¹⁶ A Co/TiO₂ catalyst was chosen as a model system as it is known for its capability of CO bond activation,² and because TiO₂ is a known photocatalyst.¹⁸ In addition, the importance of the active phase is reported for cobalt-supported catalysts: depending on the support used, cobalt oxide or metallic cobalt are believed to be more active for CO₂ hydrogenation.^{2,4} The type of active phase is believed to determine the reaction mechanism: a direct dissociation pathway or a hydrogen-assisted pathway have been reported for metallic and oxidic cobalt, respectively.² We provide evidence that UV light irradiation during CO₂ hydrogenation induces a reduction of the cobalt nanoparticles, making use of X-ray absorption spectroscopy (XAS). Furthermore, using *operando* diffuse reflectance Fourier transform spectroscopy (DRIFTS), we found enhanced catalytic performance under UV light illumination, and a concomitant change in the type and surface coverage of the reaction intermediates involved.

Results and discussion

We synthesized Co/TiO₂ catalyst materials using the incipient wetness impregnation (IWI) method. A second batch was prepared following the same procedure after the initial material was exhausted and apart from their weight loading have only minor physio-chemical differences. The two catalyst batches contained 8.7 and 6.7 wt% cobalt as determined by inductively coupled plasma-atomic emission spectrometry (ICP-AES) analysis, with surface areas of 45 and 46 m² g⁻¹ respectively, and pore volumes of ~0.25 cm³ g⁻¹ as determined by using N₂ physisorption.

The physicochemical properties of the catalyst materials were characterized using X-ray diffraction (XRD), transmission electron microscopy energy-dispersive X-ray (TEM-EDX), X-ray absorption spectroscopy (XAS), and H₂ temperature programmed reduction (TPR) (Fig. S1–S3, and Table S1). The TPR measurements indicate that partial

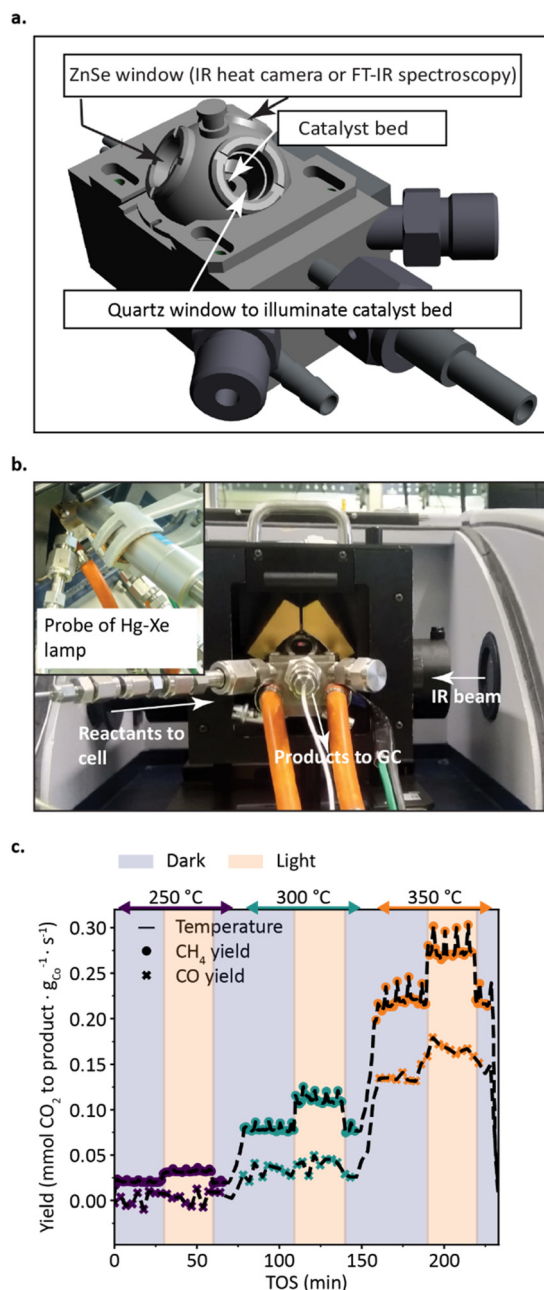


Fig. 1 Experimental approach to study the effect of UV light irradiation on a Co/TiO₂ catalyst (8.7 wt%) during CO₂ hydrogenation. a. Technical drawing and b. photograph of the Harrick cell used for the light-assisted catalysis, *operando* infrared (IR) spectroscopy experiments performed herein, showing the probe and a quartz UV-transparent window used to shine the light on the catalyst bed, and the two IR transparent windows used to measure IR spectra. The cell was connected to a gas inlet after which the gassed flow through the catalytic bed to the outlet. At the outlet reaction products were analyzed online using a gas chromatograph (GC). c. Yield of CH₄ and CO in the CO₂ hydrogenation reaction over Co/TiO₂ (8.7 wt%) at different temperatures, alternating between dark, light and dark again. Methane yield spikes result from the GC injection procedure. Conditions: the irradiance used was 208 mW cm⁻² (Hg-Xe lamp). The flow was 40 mL min⁻¹ with a ratio of CO₂:H₂:He = 4:16:20 and a gas hourly space velocity (GHSV) of 2 × 10⁵ h⁻¹.



reduction of cobalt oxide occurred around 320 and 291 °C, while further reduction towards metallic cobalt happened around 455 and 435 °C, for the 8.7 and 6.7 wt% batches respectively. The ratio of oxidic and metallic catalyst was evaluated using XAS for the 6.7 wt% Co/TiO₂ catalyst. After 1 h at 450 °C in reducing conditions, which showed the catalyst material contained 13 ± 0.7% CoO and 87 ± 0.5% of metallic Co (Table S2).

The two catalyst materials were tested under CO₂ hydrogenation conditions in the dark or under illumination using a Hg-Xe lamp with two filters (overall transmittance from 350 to 400 nm), used to prevent IR and deep UV related heating, resulting in intense bands at ~365 and ~405 nm (Fig. S2). Based on UV-vis diffuse reflectance spectroscopy (DRS) of our Co/TiO₂ catalyst materials, both titania and cobalt can be excited by the Hg-Xe lamp used (Fig. S2d). A Harrick cell (Fig. 1a and b) was used to test the catalyst materials and perform *operando* diffuse reflectance Fourier transform spectroscopy (DRIFTS) experiments, with online product analysis *via* gas chromatography (GC). The dome of the Harrick cell was equipped with two ZnSe IR transparent windows, which were used for DRIFTS, and allowed to follow the temperature of the catalyst surface using an IR heat camera. The third window in the front was a quartz, UV-vis transparent window, used to excite the catalyst with light for photo-assisted catalysis. The cell was equipped with a thermocouple inside the catalyst bed to control the catalyst temperature and the outlet of the cell was connected to a GC instrument for online product analysis.

The synthesized Co/TiO₂ catalyst material (8.7 wt%) was tested under CO₂ hydrogenation reaction conditions in the Harrick cell, both in the dark and under illumination, at reaction temperatures of 250, 300 and 350 °C. The resulting yield profile is shown in Fig. 1c. The spikes observed for the methane yield are a result of simultaneous injection for both columns. This effect is common to all yield profiles presented in this study.

UV illumination induced increases in both CH₄ and CO yields, with the CH₄ yield rising by 48, 37 and 22% and the CO yield rising by 34, 22 and 20% at 250, 300 and 350 °C, respectively. For example, the CH₄ yield increased from 0.17 mmol g_{Co}⁻¹ s⁻¹ in the dark to 0.21 mmol g_{Co}⁻¹ s⁻¹ under UV illumination and the CO yield increased from 0.10 mmol g_{Co}⁻¹ s⁻¹ to 0.12 mmol g_{Co}⁻¹ s⁻¹ from dark to light at 350 °C. Thus, UV illumination increased the CH₄ and CO yields with the largest effect at 250 °C. To better understand these effects, we investigated the effect of UV light on the catalyst material, the surface species during reaction and the temperature of catalyst.

Effect of UV light irradiation during CO₂ hydrogenation on cobalt oxidation state and particle size

To investigate the effect of UV irradiation on the active phase of Co, we used *ex situ* X-ray absorption spectroscopy (XAS) on the catalyst after performing the reaction in a Harrick cell either in the dark and under illumination, and with or without pre-reduction. The corresponding XAS data is shown in Fig. 2. To analyse the Co oxidation state present after the different treatments, we used linear combination fitting,

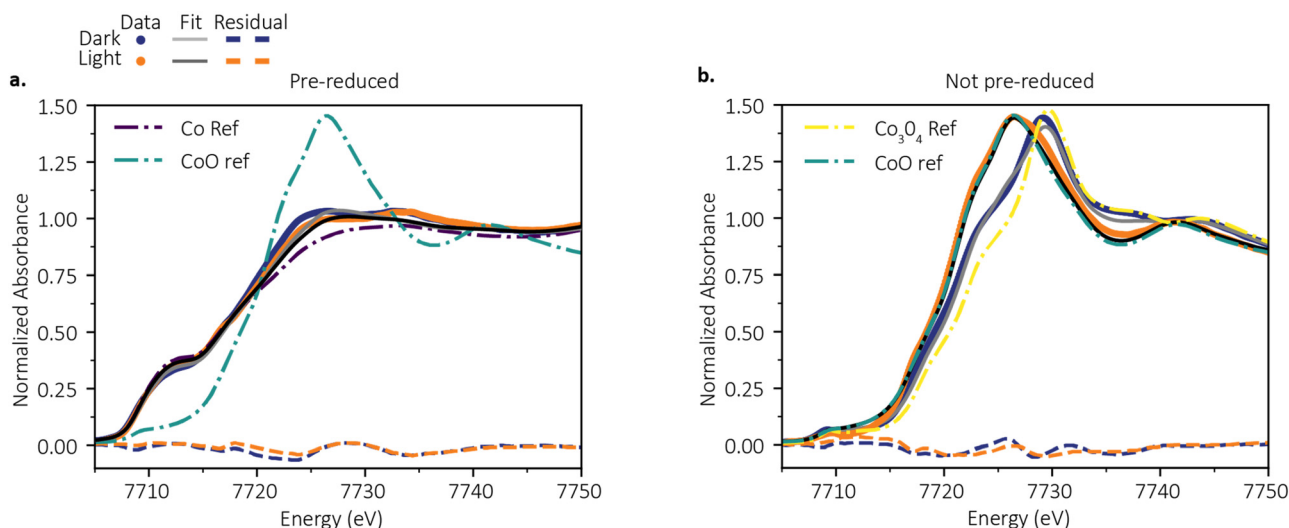


Fig. 2 Changes in the cobalt oxidation state of a Co/TiO₂ catalyst (6.7 wt%) induced by UV light irradiation, as shown by X-ray absorption spectroscopy (XAS). XAS data of the catalyst after performing the CO₂ hydrogenation reaction at 250 °C for 1 h with and without light irradiation, including reference spectra of cobalt (oxides); after reduction at 450 °C a. and without pre-reduction b. after reduction, reaction and reaction under illumination, the relative abundances found using linear combination fitting of metallic cobalt were 87 ± 0.5, 84 ± 0.5 and 91 ± 0.4%, respectively; those of CoO were 13 ± 0.7, 16 ± 0.7 and 9.3 ± 0.6% and those of Co₃O₄ were 0 ± 0.4–0.6%. Reaction *without* pre-reduction in the dark and under illumination resulted in 0% metallic cobalt; 36 *versus* 94% of CoO; and 64 *versus* 6% of Co₃O₄. The irradiance used was 1 × 10² mW cm⁻² (Hg-Xe lamp). The flow used was 40 mL min⁻¹, with a ratio of CO₂:H₂:N₂ = 4:16:20, and a gas hourly space velocity (GHSV) of 1 × 10⁵ h⁻¹.



Table 1 Linear combination fitting results for the X-ray absorption spectroscopy (XAS) data obtained for a Co/TiO₂ catalyst (6.7 wt%) after H₂ reduction, and after 1 h of CO₂ hydrogenation. The percentages of Co₃O₄, CoO and Co in the catalyst material after pre-reduction, after pre-reduction and reaction at 250 °C for 1 h with and without light, and after reaction (without pre-reduction) at 250 °C for 1 h with and without light are shown. Note that the percentages do not always add up to 100% due to rounding errors. The irradiance used was 1×10^2 mW cm⁻² (Hg-Xe lamp). The flow used was 40 mL min⁻¹, with a ratio of CO₂:H₂:N₂ = 4:16:20, and a gas hourly space velocity (GHSV) of 1×10^5 h⁻¹

	Reduced catalyst		Pre-reduced, after reaction		Not pre-reduced, after reaction	
	After reduction		Dark	Light	Dark	Light
Co ₃ O ₄ (%)	0 ± 0.6		0 ± 0.6	0 ± 0.4	64 ± 0.6	5.9 ± 0.5
CoO (%)	13 ± 0.7		16 ± 0.7	9.3 ± 0.6	36 ± 0.6	94 ± 1
Co (%)	87 ± 0.5		84 ± 0.5	91 ± 0.4	0 ± 0.4	0 ± 0.4
R factor	2×10^{-3}		2×10^{-3}	1×10^{-3}	1×10^{-3}	2×10^{-3}

using Co, CoO and Co₃O₄ as standards for every X-ray spectrum. The relative abundances found using linear combination fitting of metallic cobalt were 87 ± 0.5 , 84 ± 0.5 and $91 \pm 0.4\%$ for the pre-reduced catalyst, pre-reduced catalyst after reaction, and pre-reduced catalyst after reaction under illumination, respectively; those of CoO were 13 ± 0.7 , 16 ± 0.7 and $9.3 \pm 0.6\%$, and those of Co₃O₄ were 0 ± 0.4 – 0.6% (Table 1). This shows that cobalt gets oxidized during the reaction, while it gets reduced when it is illuminated with UV light during the reaction. To further highlight the reducing power of UV light on the state of cobalt during the reaction, we repeated the reaction under the same conditions *without* pre-reduction in the dark and under illumination, where the catalyst contained no metallic cobalt. The percentage of CoO changed from 36 ± 0.6 after reaction in the dark, to $94 \pm 1\%$ after reaction under illumination, while the Co₃O₄ percentage was 64 ± 0.6 vs. $5.9 \pm 0.5\%$. Therefore, we conclude that UV light illumination during CO₂ hydrogenation causes a reduction of cobalt in Co/TiO₂ under the conditions used herein.

To determine whether light irradiation during reaction had an effect on the cobalt particle size, we measured XRD of the fresh and used catalysts after reaction under dark or light irradiation (Fig. S4). Using the Scherrer equation, we found crystalline domains of 15, 5 and 3 nm for the fresh, used (dark) and used (light) catalyst, respectively. Furthermore, we used scanning transmission electron microscopy-energy dispersive X-ray spectroscopy (STEM-EDX, Fig. S4) to measure the cobalt nanoparticle size in the three catalysts. For each catalyst we analyzed at least a hundred particles and used several images. We found oblong cobalt particles with major diameters of 17 ± 7 , 6 ± 2 , and 5 ± 2 nm, and minor diameters of for 13 ± 5 , 4 ± 1 and 3 ± 1 nm for the fresh, spent (dark) and spent (light) catalyst, respectively. The results show a decrease in particle size after reaction, indicating a redistribution of the cobalt during the pretreatment and/or reaction. The difference between spent catalyst after reaction in the dark and under illumination were negligible, showing light does not affect cobalt particle size.

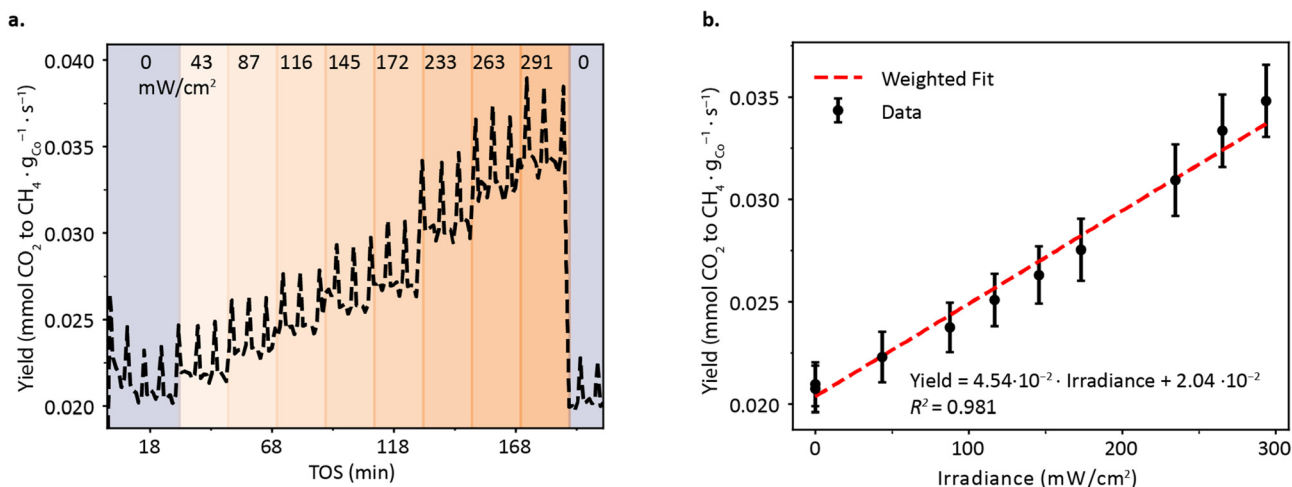


Fig. 3 CO₂ hydrogenation catalytic performance of a Co/TiO₂ catalyst (8.7 wt%) as a function of UV irradiance. a. CH₄ yield during CO₂ hydrogenation over an 8.7 wt% Co/TiO₂ catalyst plotted over time on stream under dark conditions and under different illuminations (43, 87, 116, 145, 172, 233, 263 and 291 mW cm⁻²), followed by dark (0 mW cm⁻²) again, as indicated by the shaded areas. Methane yield spikes result from the GC injection procedure. The reaction was performed at 250 °C, the flow used was 40 mL min⁻¹, with a ratio of CO₂:H₂:He = 4:16:20, and a gas hourly space velocity (GHSV) of 2×10^5 h⁻¹. b. The average CH₄ yield per irradiance from panel a. as function of irradiance. The trend in yield with irradiance was linearly fitted using a weighted fit resulting in the function: yield (mmol) = 4.54×10^{-2} (mmol mW⁻¹) × Irradiance (mW) + 2.04×10^{-2} (mmol) ($R^2 = 0.981$).



To further understand the effect of UV light irradiation on the CO₂ hydrogenation reaction we performed activity, DRIFTS and IR thermometry experiments.

Effect of UV light irradiation on the catalytic CO₂ hydrogenation performance

To examine the influence of UV irradiation on the CH₄ yield during CO₂ hydrogenation, we measured the yield as function of irradiance at 250 °C (Fig. 3). We found a linear correlation between catalytic activity and irradiance, with $R^2 = 0.981$. Such linearity of reaction rate with irradiance is sometimes used as evidence for photochemical effects, as opposed to purely photothermal effects, where the rate is expected to exponentially increase with temperature (Arrhenius type behavior). However, alternative explanations have been proposed in literature, and the method is not conclusive when the temperature difference is small.^{19,20}

To test whether the reaction kinetics for CO and CH₄ production were affected by UV irradiation, we determined the apparent activation energies of the reaction towards CH₄ and CO₂ with and without illumination using Arrhenius plots (Fig. 4). To extract values for apparent activation energies, we linearly fitted the data points below 300 °C, where the conversion was below 10%, and thus mass-transfer effects are expected to be negligible. Under dark conditions, the apparent activation energies were 71 kJ mol⁻¹ for CH₄ (E_{a,CH_4}), and 110 kJ mol⁻¹ for CO ($E_{a,CO}$), while under UV illumination, they were 73 kJ mol⁻¹ for CH₄, and 145 kJ mol⁻¹ for CO. For the reaction towards CH₄, the activation energies were comparable. On the other hand, the activation energies for CO in the dark *versus* under illumination were different, suggesting an inhibiting effect of light on the production of CO during CO₂ hydrogenation over Co/TiO₂. Nonetheless, one should exercise caution in interpreting these trends, as

the R^2 values for $E_{a,CO}$ were 0.85 and 0.90, due to low CO yield. Furthermore, we have calculated the CH₄ and CO selectivity obtained during the Arrhenius experiments (Fig. S5). The effect of light on selectivity was negligible in these experiments, potentially because only the surface was illuminated while bulk activity dominated the measured activity.

The influence of UV irradiation on surface intermediates during CO₂ hydrogenation

To better understand the effect of the UV irradiation on the reaction mechanism of Co/TiO₂ catalysts during CO₂ hydrogenation, we used *operando* diffuse reflectance infrared Fourier transform spectroscopy (DRIFTS) with online product analysis using a GC. First, we performed an isothermal experiment in *duplo*, in which a Co/TiO₂ catalyst was kept under CO₂ hydrogenation conditions in the dark or under illumination at 250 °C for 5 h (Fig. 5, S6 and S7), similar to what was done for the *ex situ* XAS analysis. In both cases, we observed IR bands at 1990–1980 cm⁻¹, which are characteristic of CO* adsorbed on Co,² and IR bands at 1565 and 1375 cm⁻¹, which we assigned to formate species (COO asymmetric and COO symmetric stretching modes, respectively, with the latter band also containing a CH bending vibration).^{2,18} Both CO* and formate species are known surface intermediates in the CO₂ hydrogenation reaction over Co/TiO₂ catalysts.^{2,15} Furthermore, IR bands were observed at ~1620 cm⁻¹, typical for adsorbed water (which is a byproduct of CO₂ methanation), and at ~1440 cm⁻¹, which is typically ascribed to the presence of bicarbonate species.¹⁸

Such isothermal experiments show that UV light influences the type of adsorbates which are accumulating on the surface of a Co/TiO₂ catalyst under reaction conditions.

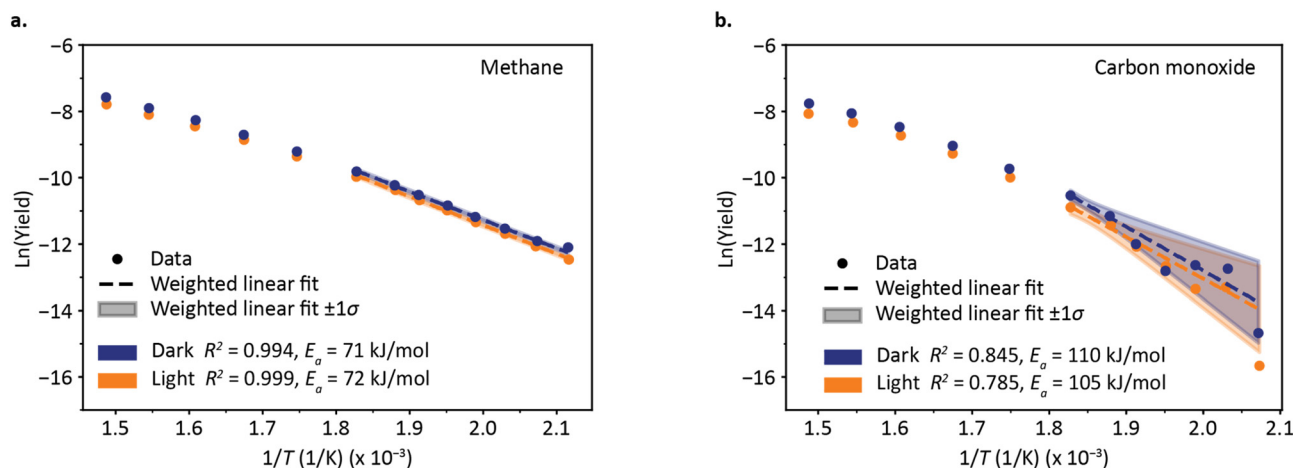


Fig. 4 Catalytic activity as a function of temperature with and without illumination. Arrhenius plots of CO₂ hydrogenation over a 6.7 wt% Co/TiO₂ catalyst with and without illumination of a. CH₄ ($E_{a,dark} = 71$ and $E_{a,light} = 72$ kJ mol⁻¹) and b. CO ($E_{a,dark} = 110$ and $E_{a,CO} = 105$ kJ mol⁻¹). The points represent data, the dotted lines a weighted linear fit and the shaded areas the error of the fit ($\pm 1\sigma$). Conditions: the irradiance used was 130 mW cm⁻² (Hg-Xe lamp). The flow used was 40 mL min⁻¹, with a ratio of CO₂:H₂:He = 4:16:20, and a gas hourly space velocity of 2.1×10^5 h⁻¹ and 1.5×10^5 h⁻¹ for with and without illumination respectively.



In particular, the accumulation of bicarbonate species over time was prevented by irradiation, as shown by the trend in IR band areas for the two experiments (Fig. 6d). For the *duplo* experiment the data points from the first 75 points were left out, as the area was zero. Moreover, the area and band position of CO* and formate species were significantly affected by irradiation (Fig. 6a and b). The CO* area increased slightly over time both with and without illumination, and under illumination the peak area was bigger during the first experiment while lower during the *duplo* experiment. A decrease in CO* area upon illumination was also observed when the light was turned on and off within one experiment (Fig. 7b). We note that the trends in peak area and position were substantially influenced by the pretreatment (*e.g.*, whether the catalyst is illuminated from before or only the start of the flow of reaction gasses) and the type of carrier gas might also have an influence (N₂ vs. He, due to their different heat capacity). The CO* IR band position in the dark red-shifted from ~ 1983 to ~ 1978 cm⁻¹ in ~ 60 min and stabilized around these values. Under illumination, the CO* IR band position was remarkably stable at ~ 1975 cm⁻¹. The formate IR bands under both dark and illumination grew rapidly in the first minutes, and then slowly increased in intensity with a similar slope, but with different overall intensity. This indicates a lower surface coverage of formates under light irradiation, under the assumption that the species have the same extinction coefficient in dark and under illumination.

As both bicarbonate and formate species are considered to be surface intermediates in the CO₂ reduction reaction towards CH₄,¹⁵ the lower coverage of these species could indicate that light promotes further reaction towards CH₄. However, the lower surface coverage upon UV illumination could also indicate an inhibition of the formation of formate

and bicarbonate species. Future modulation excitation (ME) experiments with IR spectroscopy could provide clarification in the distinguishing between the two.

To further analyse the effect of UV irradiation on the CO* coverage, we performed an experiment where the Co/TiO₂ catalyst was tested for CO₂ hydrogenation in the dark for 30 min, followed by light (30 min), and dark again (10 min) at 250, 300 and 350 °C (Fig. 7a). The CO₂ hydrogenation yield increased with temperature and upon UV illumination and reverted back when the illumination was stopped (Fig. 1c). To analyse the DRIFTS data, we fitted the CO* IR band with a Gaussian function, and extracted the peak position and peak area, which is plotted over time-on-stream (TOS, Fig. 7b). A peak at 1305 cm⁻¹, corresponding to a CH bending mode,²¹ is assigned to methane. In the dark, the CO* IR band position started at 1975 cm⁻¹ and shifted by ~ 5 cm⁻¹ to lower wavenumbers under illumination. When the light was turned off, the band position reverted to higher wavenumbers, and with increasing TOS, it exhibited a slight shift toward higher wavenumbers. Similarly, the integrated area of the CO_{ad} band increased over time and decreased reversibly under illumination. These observations are mostly consistent with observations made during the isotherm experiments for 5 h with and without light (Fig. 5 and 6), albeit the absolute peak position and areas differ. Additionally, the formate band areas under illumination were much lower compared to the CO₂ methanation reaction in the dark, and the peak assigned to bicarbonate for the dark reaction was not visible under UV illumination.

The observed decrease in intensity and shift in CO IR band to lower wavenumbers is consistent with a decrease in CO* coverage due to illumination, leading to a shift of the IR band to lower wavenumbers due to reduced vibrational coupling among adsorbed CO* molecules.²² In addition, the

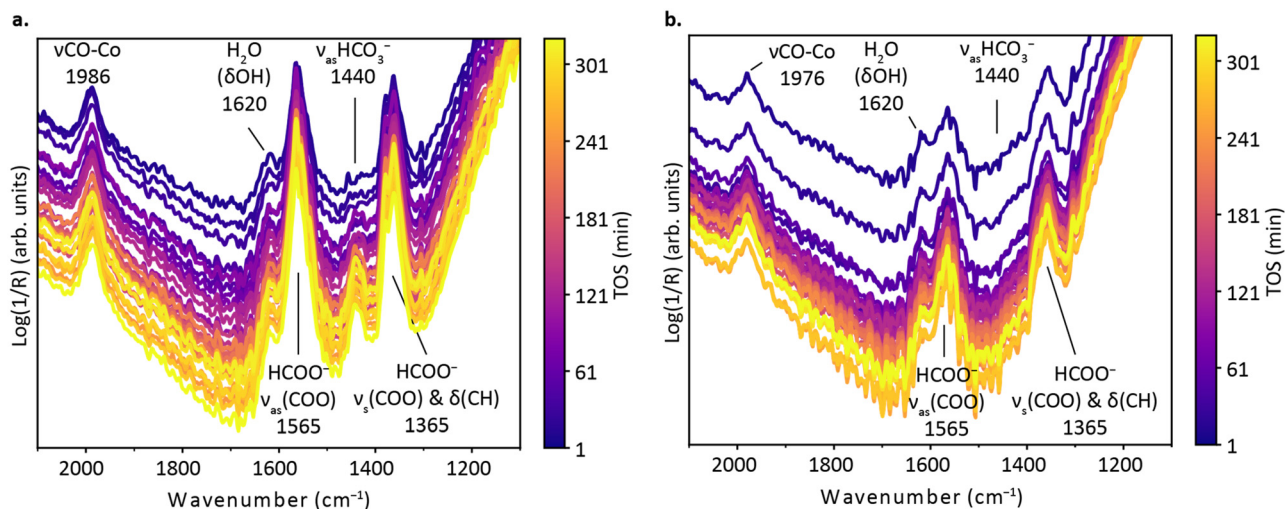


Fig. 5 Changes in CO₂ hydrogenation reaction intermediates over a Co/TiO₂ catalyst (8.7 wt%) induced by light observed by *operando* diffuse reflectance infrared Fourier transform spectroscopy (DRIFTS). a. and b. DRIFT spectra taken during CO₂ hydrogenation reaction over a Co/TiO₂ catalyst over time (dark vs. light, respectively). Conditions: the irradiance used was 208 mW cm⁻² (Hg-Xe lamp). The flow used was 40 mL min⁻¹, with a ratio of CO₂ : H₂ : N₂ = 4 : 16 : 20 and a gas hourly space velocity (GHSV) of 2×10^5 h⁻¹, respectively.



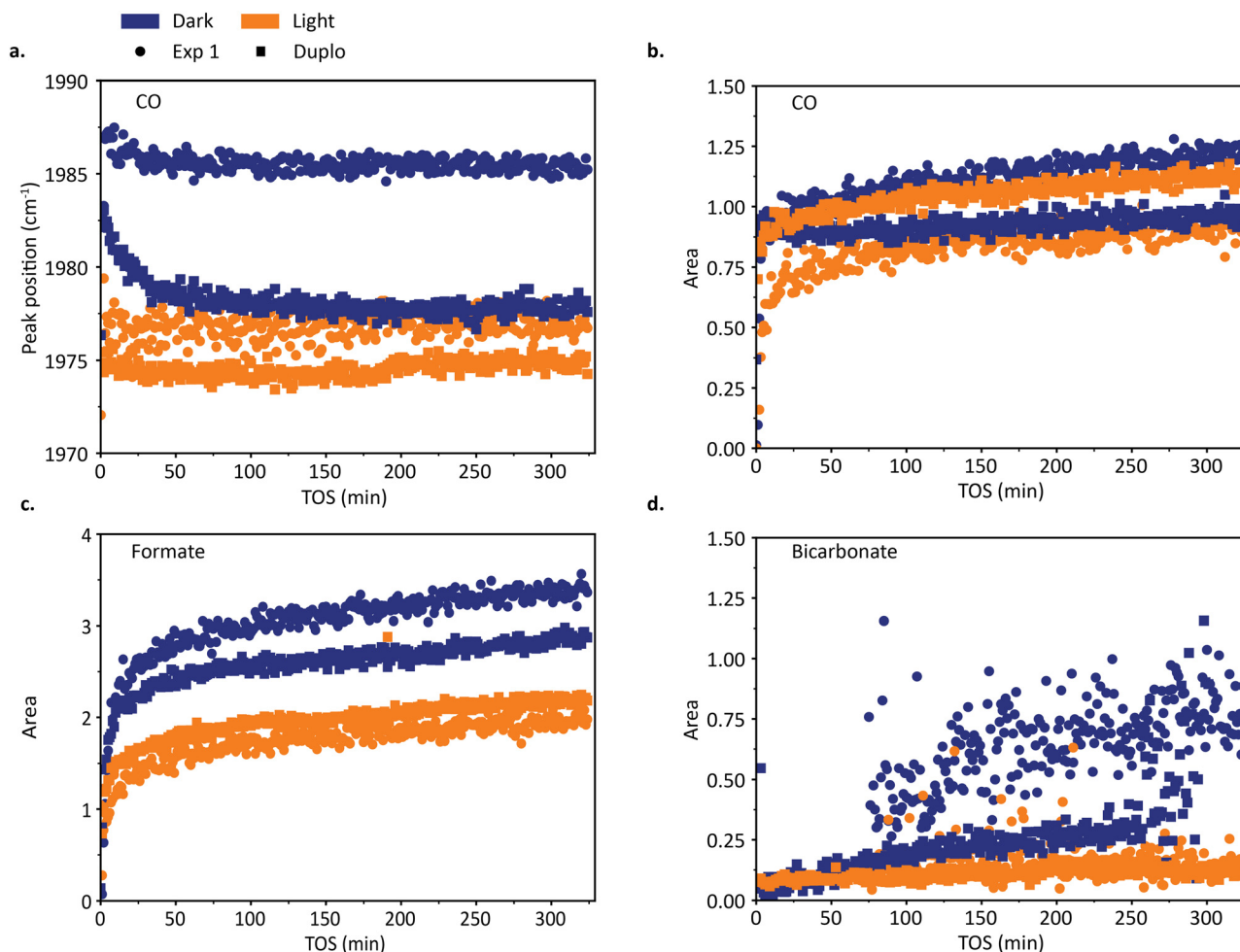


Fig. 6 Evolution of the CO peak position and the CO, formate and bicarbonate peak area of the infrared bands with increasing time-on-stream (TOS) during CO₂ hydrogenation over a Co/TiO₂ catalyst (8.7 wt%). Parameters extracted from the diffuse reflectance infrared Fourier transform spectroscopy (DRIFTS) data taken during CO₂ hydrogenation in dark and under illumination (208 mW cm⁻²). a. The peak position of CO*. b. The peak area of CO, c. formate (1360 cm⁻¹) and d. the peak area of bicarbonate (1440 cm⁻¹).

decreased band intensity is consistent with a lowered coverage. Therefore, we assign the changes of the CO* IR band to a decreased CO* coverage on the cobalt metal nanoparticle surface upon illumination. We note that the observed shift in CO IR bands could alternatively be explained by an electron excitation to an antibonding orbital of CO* resulting in a lower C–O bond energy, which would result in a red shift of the CO* band. However, such excited states are short lived (femto- to picosecond timescales) compared to average photon absorption rates (one photon per millisecond).^{23,24} Therefore, while we cannot exclude the formation of such states, their time-averaged population is expected to be too low to be detected using our FTIR method (one spectrum per minute). The decrease in CO coverage upon UV irradiation can be explained by several phenomena, such as photothermal effects, electron transfer or changes in the catalyst material. Since the change in the CO* IR band upon illumination was fast and reversible, while the observed changes in Co oxidation state were irreversible (*ex situ* XAS data, Fig. 2), the two phenomena are not correlated.

To investigate whether our observations could be resulting from photothermal effects, we measured the apparent temperature at the surface of a Co/TiO₂ catalyst (6.7 wt%) during CO₂ hydrogenation reaction in the dark and under illumination using an IR heat camera. IR images of the Co/TiO₂ catalyst bed were taken during CO₂ hydrogenation set at 300 °C through the ZnSe window of the Harrick cell with and without illumination (Fig. 8a and b). We observed a slight temperature gradient in the catalyst bed under dark conditions, and an increase in apparent temperature when turning on the light (Fig. 6c). When the UV light was turned on, the apparent temperature increased from 300 to 330 °C, and within seconds it stabilized to 320 °C. Thus, the temperature difference at the surface of the catalyst bed caused by illumination was estimated to be ~20 °C. On the other hand, the temperature measured with a thermocouple placed under the catalyst bed changed by a maximum of only 0.5 °C at the used irradiance (<160 mW cm⁻²). This shows that a temperature gradient is formed in the catalyst bed, as the light only affects the (sub-)surface of the catalyst material.



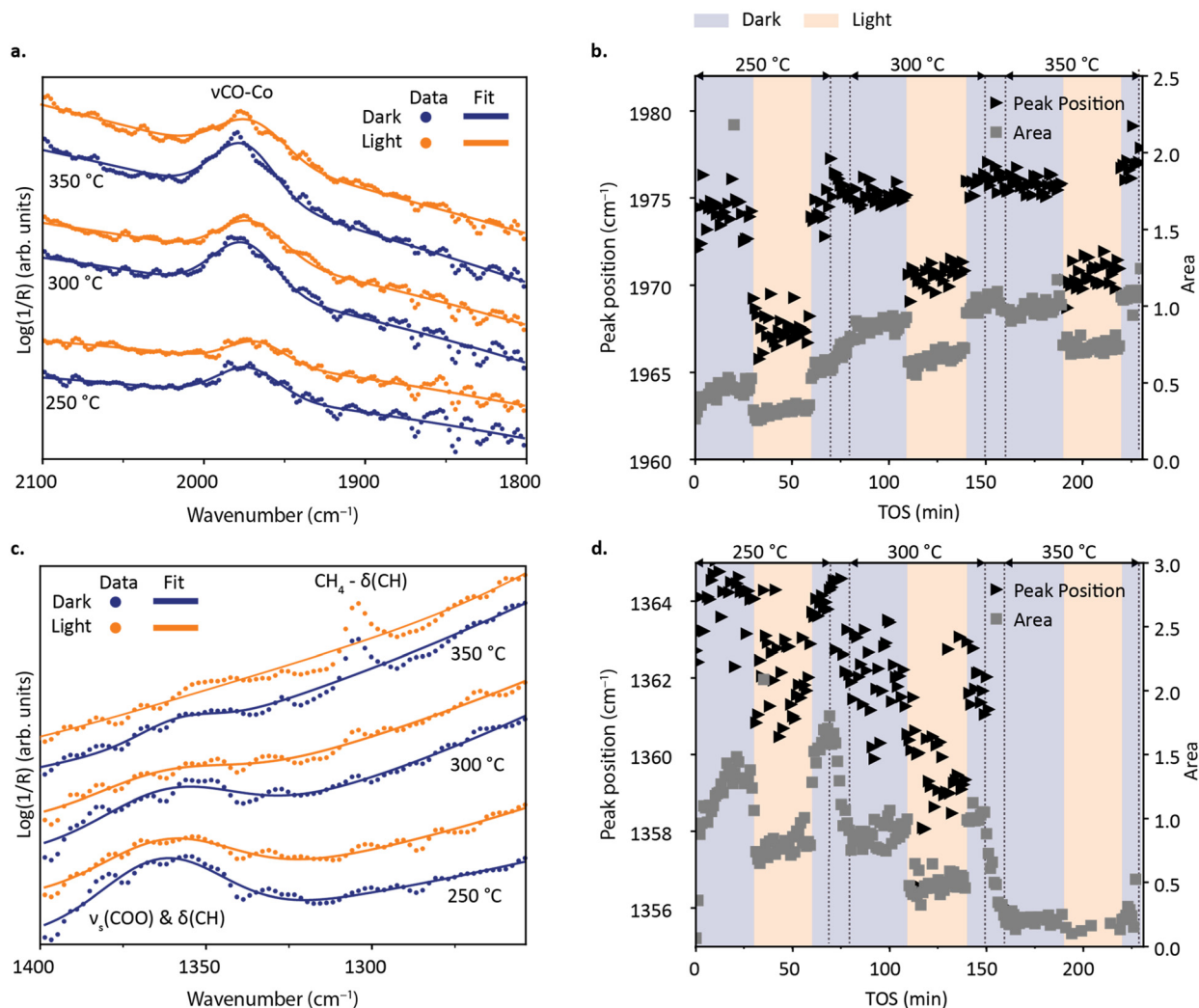


Fig. 7 The effect of UV irradiation on adsorbed CO intermediates on a Co/TiO₂ catalyst (8.7 wt%). a. Diffuse reflectance infrared Fourier transform spectroscopy (DRIFTS) data taken during the dark and under illumination (208 mW cm⁻², Hg-Xe lamp) at 250, 300, and 350 °C fitted with a Gaussian function. b. The peak position and peak area of CO_{ad} as function of time-on-stream (TOS), as extracted from the Gaussian fit, where the blue and orange area indicates when light off and on respectively. c. and d. The same as a. and b. but for formate, for which the 1360 cm⁻¹ peak was fitted. The flow used was 40 mL min⁻¹, with a ratio of CO₂ : H₂ : He = 4 : 16 : 20, and a gas hourly space velocity (GHSV) of 2 × 10⁵ h⁻¹.

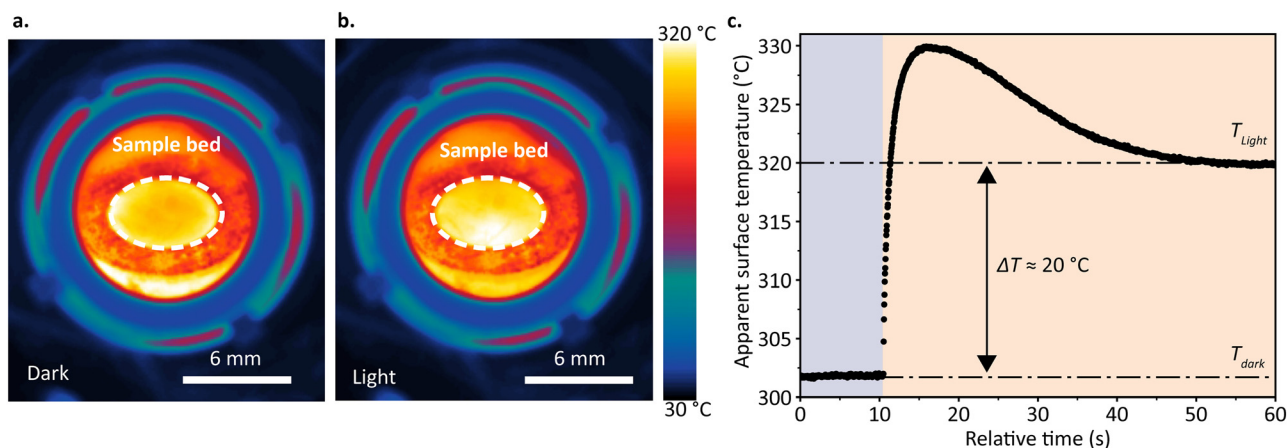


Fig. 8 Photothermal effects of light irradiation revealed by an infrared camera. a. Infrared image of an 8.7 wt% Co/TiO₂ catalyst bed under dark conditions and b. irradiation with 160 mW cm⁻² (Hg-Xe lamp) during CO₂ hydrogenation over Co/TiO₂ at 300 °C set temperature, showing the apparent surface temperature in the reactor, and its change upon irradiation. c. The temperature of the catalyst bed measured over time. When turning opening the shutter and illuminating the catalyst bed a temperature increase of 20 °C was measured. A total flow of 40 mL min⁻¹ with a ratio of CO₂ : H₂ : He = 4 : 16 : 20 was used (with a gas hourly space velocity (GHSV) of 2 × 10⁵ h⁻¹).



It should be noted that the spatial resolution of the IR heat camera is not high enough to capture nanoscale photothermal effects, therefore we suggest the use of photoluminescence thermometry in future studies.

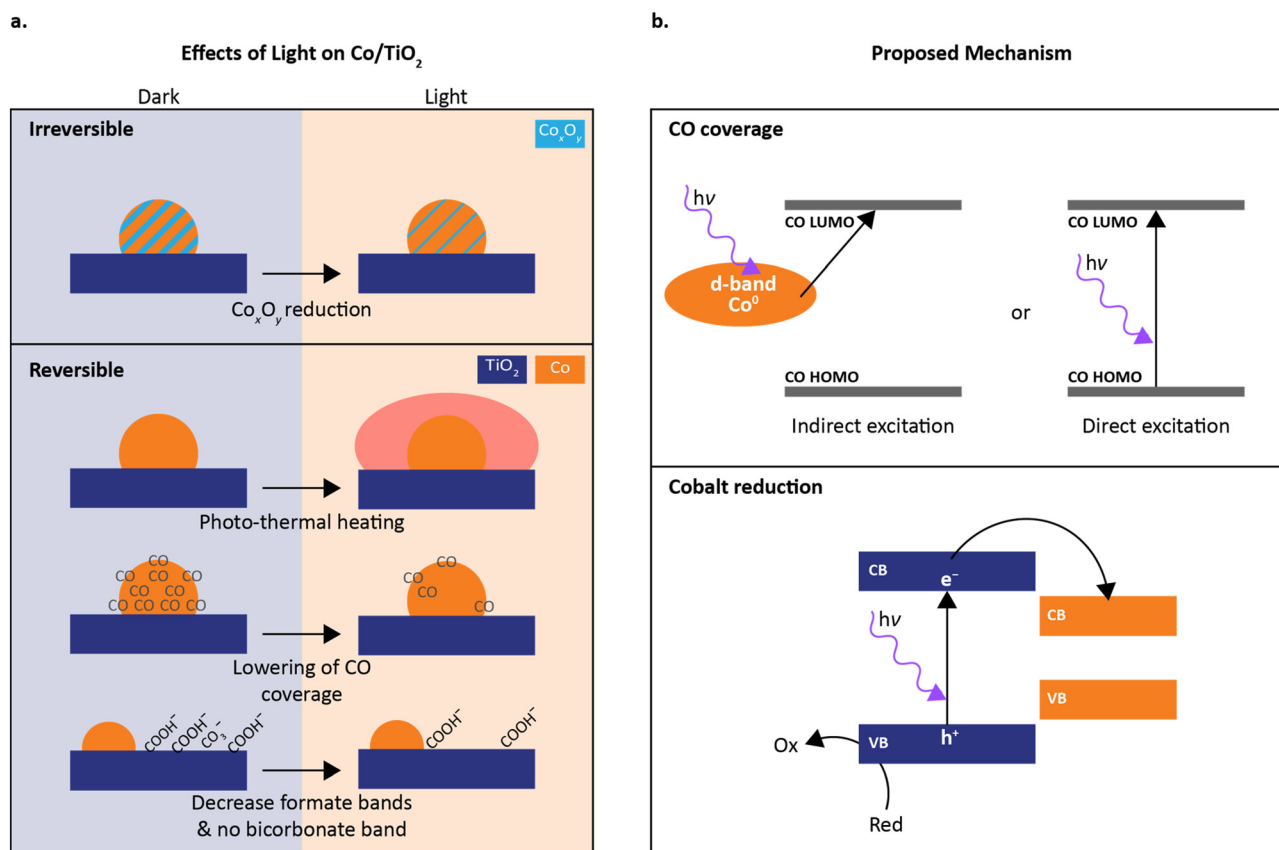
The temperature increase of 20 °C observed with the IR camera cannot explain the change in CO* surface coverage, because the CO* IR band area and position are comparable at 250 and 350 °C in the dark, yet decrease significantly when the catalyst is illuminated with UV light. Therefore, we conclude that the observed effect of light on CO* surface coverage is not thermal, but is instead related to photo-induced charge transfer. Notably, light illumination was shown to induce CO desorption from a Pt/Al₂O₃ catalyst at lower temperatures. This effect was rationalized by photoexcitation of the Pt–CO bond and a subsequent transfer of energy to vibrational states, resulting in enhanced CO desorption.²⁵

In contrast, the IR imaging results in our work suggest that the effect of UV light illumination on the catalytic activity may be mostly thermal. To estimate the photothermal effect of irradiation, we can use the determined apparent activation energies (Fig. 4) to calculate

the change in rate with temperature and compare this to the observed reaction rate. When plugging in $\Delta T \approx 20$ °C into the rate equation we get:

$$\frac{k_{\text{light}}}{k_{\text{dark}}} \approx 1.7$$

where k_{light} and k_{dark} are the rate constant under UV irradiation and in dark, respectively, meaning that heating by light can account for up to a 1.7-fold increase in activity. In addition, using the fit from the Arrhenius test conducted in the dark (Fig. 4), we calculated the effect of a 20 °C temperature increase (from 250 to 270 °C) on the activity under dark. The results indicate that the activity increases by ~1.8-fold for methane. When considering the temperature difference measured in the bulk (0.5 °C), the expected rate enhancement is ~1.04. Notably, we expect a rate increase of 1.4 under illumination (160 mW cm⁻²) using the fit from Fig. 3b (which was at 250 °C). Thus, while the bulk temperature increase does not account for the observed rate increase, the temperature difference at the surface would be sufficient to explain the change in activity.



Scheme 1 Mechanistic insights into the effect of UV light on Co/TiO₂ for catalytic CO₂ hydrogenation. a. Schematic summary of the effects observed upon illumination divided by reversible effects (*i.e.*, photothermal heating, CO desorption and other intermediate changes) and irreversible effects (*i.e.*, reduction of cobalt). b. Schematic representation showing the proposed mechanism for CO desorption *via* indirect excitation from the metal to the lowest unoccupied molecular orbital (LUMO) of CO* or direct excitation within the CO* from the highest occupied molecular orbital (HOMO) to the LUMO, and the proposed charge transfer mechanism underlying photo-induced Co reduction, where electrons from titania get excited to the conduction band and transfer to cobalt oxide.



To further understand and quantify photothermal effects on catalytic performance, future studies will focus on modelling the temperature gradients along the depth of the catalyst bed under both dark and illumination conditions.

Discussion

We observed several effects of UV light on the catalysis and catalyst material, as summarized in Scheme 1a. We identified two main effects on Co/TiO₂ catalysts resulting from UV illumination during CO₂ hydrogenation: (i) cobalt reduction, and (ii) changes in (types of) surface species. The former is irreversible, while the latter is reversible, suggesting that the two effects are not related. The reduction of cobalt may in principle be explained by either an increase in temperature and thermal reduction by H₂ in the reaction mixture, or *via* a charge transfer mechanism (Scheme 1b). In the TPR, we observed a peak at 291 °C, assigned to the reduction of Co₃O₄ to CoO, and a peak at 435 °C, assigned to the reduction of CoO to Co metal.² Since the CO₂ hydrogenation reaction is performed at 250 °C and the observed increase in catalyst surface temperature upon illumination was not more than 30 °C, a thermal reduction from Co₃O₄ to CoO is considered to be possible, but the reduction all the way to Co⁰ seems unlikely. Therefore, our results suggest that heat is not solely responsible for the observed reduction of cobalt, and that a charge transfer mechanism contributes to the reduction.

We propose three hypotheses for charge transfer: a direct excitation of the cobalt oxide or a charge transfer from the titania support to the cobalt metal (oxide) nanoparticles. Another charge transfer mechanism may also occur upon light irradiation, *i.e.* cobalt intervalence charge transfers (*e.g.* electrons from Co(II) to Co(III)), which was proposed to affect catalytic performance.²⁶ In this case, the overall redox state of Co in the catalyst would remain the same, yet we observed an overall reduction of the cobalt(oxide) metal nanoparticles. Thus, this mechanism by itself cannot explain the observations we made using XAS. Furthermore, due to the mixed structure of cobalt oxide states, its electronic structure is complex and contains several states between the conduction band (CB) and the valence band (VB).²⁷ Hence, an indirect excitation *via* titania is more likely. The cobalt oxide and titania bands and their relative positions are shown in Scheme 1.^{28,29} An electron is photo-excited from the VB to the CB in the TiO₂ support, which then transfers to the CB of the cobalt oxide, resulting in a reduction. The hole left in the VB of the TiO₂ support is filled by a counter reaction at the VB.

The observed changes in CO* IR bands can be explained by CO* desorption upon UV illumination. We propose that light-induced CO* desorption is caused by either indirect excitation from the d-band of the cobalt metal to the lowest unoccupied molecular orbital (LUMO) of CO* or by direct excitation from the highest occupied molecular orbital (HOMO) to the LUMO of CO* (Scheme 1b). Such charge transfer to the LUMO of CO* induces desorption, as also

proposed in the work of Alvarez *et al.*²⁵ The relationship between photo-desorption of CO* and photo-induced charge transfer is further supported by recently developed kinetic model on photo-desorption from a Pt/Al₂O₃ catalyst. It was shown that photo-induced desorption cannot be kinetically described by adjusting the kinetic parameters for the description of thermally-driven desorption. Instead, a term to describe photo desorption independent of the thermal desorption needed to be added.²⁴ Notably, the observed decrease in CO* surface coverage upon UV illumination did not result in a change in apparent activation energy for CH₄ formation. This is consistent with the low reaction order in CO₂ and low dependency of the reaction rate on CO* surface coverage for Co/TiO₂.² On the other hand, the apparent activation energy for CO formation increased upon UV illumination. This phenomenon deserves further investigation, as it suggests that the catalyst selectivity may be tweaked between CO₂ methanation and CO production *via* reverse water gas shift (rWGS) using UV light.

Conclusions

Our study shows that the active phase of a Co/TiO₂ catalyst can be changed during the CO₂ hydrogenation reaction using UV light, and that UV illumination influences the coverage and type of CO₂ hydrogenation reaction intermediates. We observed that Co_xO_y was reduced under irradiation during CO₂ hydrogenation, which we ascribe to photo-induced charge transfer from titania to the supported metal (oxide) nanoparticles. We further report a decrease in surface coverage of CO*, formate and bicarbonate on Co/TiO₂ upon UV light illumination. We hypothesize that an additional charge-transfer mechanism, either direct or indirect, drives the observed CO* desorption under illumination. Interestingly, the improved yield and changes in reaction mechanism upon UV illumination did not correlate to the reduction of the active phase. Future studies should further test the proposed mechanism for light interaction with Co/TiO₂, explore possible effects on TiO_x overlayer formation on cobalt metal (oxide) nanoparticles, and expand the study to other supported catalyst systems as well as reaction conditions. Reactions where CO* is deemed to be poisoning, such as CO oxidation and formate decomposition, hold promise to further leverage the photo-induced desorption of CO*.

Experimental

Co/TiO₂ catalysts (6–9 wt% Co) were prepared by incipient wetness impregnation using Co(NO₃)₂·6H₂O (99%, Thermo Scientific) and P25 TiO₂ (99.5%, 50 m² g⁻¹) as support material. For this research we aimed for 10 wt% Co loading, to obtain a catalyst material similar to previous work about CO₂ hydrogenation over Co/TiO₂ (Ten Have *et al.*²). However, we obtained 8.7 and 6.7 wt% Co loading, as some of the



cobalt precursor remained on the walls of the container. To characterize the catalyst materials, we used an X-ray diffraction (Bruker D8 Advance instrument equipped with a Cu K α X-ray tube ($\lambda = 1.5418 \text{ \AA}$) operated at 40 kV and 40 mA (diffractograms were background subtracted), transmission electron microscopy-energy dispersive X-ray spectroscopy (TFS Spectra300 instrument using an acceleration voltage of 300 kV), UV-vis diffuse reflectance spectroscopy (Lambda 950S instrument), temperature programmed reduction (Altamira Instruments equipment with a temperature ramp of $5 \text{ }^\circ\text{C min}^{-1}$ under 5% H $_2$), N $_2$ physisorption (P3 Instruments Sync 400 instrument) and Mikrolab Kolbe performed the inductively coupled plasma atomic emission spectroscopy measurements. To investigate the effect of light on the reaction mechanism, we used *operando* diffuse reflectance infrared Fourier transform spectroscopy (Bruker Tensor 37 instrument) combined with a Global Analyser Solutions CompactGC 4.0 instrument for online product analysis equipped with a thermal conductivity detector (TCD) and a flame ionization detector (FID), while illuminating with a Hg-Xe lamp (Lightingcure LC8 L9566-01A by Hamamatsu equipped with a A9616-05 filter, an A10014-50-0110 light guide and an E7658-01 condenser lens) to trigger photo-assisted catalysis. The irradiances used during experiments were determined by measuring the output power of the light from the lamp (using a Thorlabs PM100D power meter and S425C sensor) and dividing that by the spot size of the light. X-ray absorption spectroscopy were collected at the SuperXAS beamline of the Swiss Light Source, Villigen, Switzerland to study the influence of light during the catalytic CO $_2$ hydrogenation reaction on the oxidation state of cobalt (fluorescence mode with PIPS detector, Si(111) monochromator in quick scan mode, Si-coated collimating mirror for higher harmonic cut-off). Before *ex situ* XAS, the catalysts were tested in CO $_2$ hydrogenation for 1 h at 250 $^\circ\text{C}$, either directly or after reduction at 450 $^\circ\text{C}$ for 1 h. The temperature was steered using an external thermocouple to allow for sample transfer to a sealed capillary in inert atmosphere *via* a glovebox. The catalyst temperature was measured with an internal thermocouple in reference experiments to be approximately 240 $^\circ\text{C}$ and 430 $^\circ\text{C}$. For XAS measurements, the catalysts were diluted with SiO $_2$ to a weight ratio of 1:9, except for the fresh catalyst which was diluted with cellulose to a weight ratio of 1:9. To determine the temperature increase of the catalytic surface induced by UV illumination, an IR heat camera was used (FLIR A700 (pixel pitch = 12 μm , FLIR lens $f = 18 \text{ mm}$ (24 $^\circ$) F/1.0). The emissivity value for the IR heat camera measurements was set to 0.62 in the FLIR Research Studio software, based on a calibration using the temperature measured by a thermocouple in the catalyst bed (Fig. S8 and Table S3). The catalyst material was reduced *in situ* at 450 $^\circ\text{C}$ in a 1:1 He:H $_2$ mixture. The reaction was performed under a 1:4:5 CO $_2$:H $_2$:He (40 mL min $^{-1}$) flow at different reaction temperatures. N $_2$ instead of He was used for the sample preparation for the X-ray absorption spectroscopy experiments. The gas hourly space

velocity was calculated by dividing the gas flow (L h $^{-1}$) by the volume of the catalyst (L). The latter was obtained by multiplying the catalyst density (g L $^{-1}$) by its mass (g).

Author contributions

D. N. Maaskant: conceptualization, data curation, formal analysis, investigation, methodology, software, visualization and writing (original draft), writing (review & editing). P. T. Prins: resources, methodology and writing (review & editing). N. S. Genz: data curation, formal analysis, investigation and writing (review & editing). B. M. Weckhuysen: project administration, resources, supervision and writing (review & editing). M. Monai: conceptualization, funding acquisition, methodology, project administration, resources, supervision and writing (review & editing).

Conflicts of interest

There are no conflicts to declare.

Data availability

Data supporting this article have been included as part of the supplementary information (SI).

Supplementary information: Fig. S1–S8, including details on physicochemical properties of the catalyst material, selectivity data, extended spectroscopic ranges, a *duplo* experiment and an emissivity sensitivity analysis. See DOI: <https://doi.org/10.1039/d5cy01557j>. The data for this article have been uploaded to the YODA repository, and are available at <https://doi.org/10.24416/UU01-VHI2DA>.

Acknowledgements

This work is part of the Advanced Research Center for Chemical Building Blocks, ARC CBBC, which is co-founded and co-financed by the Dutch Research Council (NWO) and the Netherlands Ministry of Economic Affairs and Climate Policy. We acknowledge Frank de Groot and Florian Meirer, both from Utrecht University (UU), for discussions about the X-ray absorption spectroscopy data. Mikrolab Kolbe is acknowledged for the ICP-AES measurements. We thank Savannah Turner from the Electron Microscopy Centre of Utrecht University for performing the STEM-EDX measurements. We thank the Swiss Light Source (SLS, Villigen, Switzerland) for providing beamtime at the SuperXAS beamline.

Notes and references

- 1 C. Vogt, E. Groeneveld, G. Kamsma, M. Nachtegaal, L. Lu, C. J. Kiely, P. H. Berben, F. Meirer and B. M. Weckhuysen, *Nat. Catal.*, 2018, **1**, 127–134.
- 2 I. C. ten Have, J. J. G. Kromwijk, M. Monai, D. Ferri, E. B. Sterk, F. Meirer and B. M. Weckhuysen, *Nat. Commun.*, 2022, **13**, 324.



- 3 M. J. Ledoux, C. Pham-Huu and R. R. Ghianellit, *Curr. Opin. Solid State Mater. Sci.*, 1996, **1**, 96–100.
- 4 S. Lyu, L. Wang, J. Zhang, C. Liu, J. Sun, B. Peng, Y. Wang, K. G. Rappé, Y. Zhang, J. Li and L. Nie, *ACS Catal.*, 2018, **8**, 7787–7798.
- 5 M. Ronda-Lloret, G. Rothenberg and N. R. Shiju, *ChemSusChem*, 2019, **12**, 3896–3914.
- 6 Y. P. Pei, J. X. Liu, Y. H. Zhao, Y. J. Ding, T. Liu, W. Da Dong, H. J. Zhu, H. Y. Su, L. Yan, J. L. Li and W. X. Li, *ACS Catal.*, 2015, **5**, 3620–3624.
- 7 C. J. Pan, M. C. Tsai, W. N. Su, J. Rick, N. G. Akalework, A. K. Agegnehu, S. Y. Cheng and B. J. Hwang, *J. Taiwan Inst. Chem. Eng.*, 2017, **74**, 154–186.
- 8 Y. Xie, J. Wen, Z. Li, J. Chen, Q. Zhang, P. Ning and J. Hao, *ACS Mater. Lett.*, 2023, **5**, 2629–2647.
- 9 S.-W. Ho, J. M. Cruz, M. Houalla and D. M. Hercules, *J. Catal.*, 1992, **135**, 173–185.
- 10 M. Shetty, A. Walton, S. R. Gathmann, M. A. Ardagh, J. Gopeesingh, J. Resasco, T. Birol, Q. Zhang, M. Tsapatsis, D. G. Vlachos, P. Christopher, C. D. Frisbie, O. A. Abdelrahman and P. J. Dauenhauer, *ACS Catal.*, 2020, **10**, 12666–12695.
- 11 A. V. Puga, *Catal. Sci. Technol.*, 2018, **8**, 5681–5707.
- 12 K. Ahmad and S. Upadhyayula, *Environ. Prog. Sustainable Energy*, 2018, **38**, 98–111.
- 13 C. Kim, S. Hyeon, J. Lee, W. D. Kim, D. C. Lee, J. Kim and H. Lee, *Nat. Commun.*, 2018, **9**, 3027.
- 14 B. Xie, R. J. Wong, T. H. Tan, M. Higham, E. K. Gibson, D. Decarolis, J. Callison, K. F. Aguey-Zinsou, M. Bowker, C. R. A. Catlow, J. Scott and R. Amal, *Nat. Commun.*, 2020, **11**, 1615.
- 15 T. H. Tan, B. Xie, Y. H. Ng, S. F. B. Abdullah, H. Y. M. Tang, N. Bedford, R. A. Taylor, K. F. Aguey-Zinsou, R. Amal and J. Scott, *Nat. Catal.*, 2020, **3**, 1034–1043.
- 16 C. Hu, X. Chen, J. Low, Y. W. Yang, H. Li, D. Wu, S. Chen, J. Jin, H. Li, H. Ju, C. H. Wang, Z. Lu, R. Long, L. Song and Y. Xiong, *Nat. Commun.*, 2023, **14**, 221.
- 17 H. Chen, Z. Yang, X. Wang, F. Polo-Garzon, P. W. Halstenberg, T. Wang, X. Suo, S. Z. Yang, H. M. Meyer, Z. Wu and S. Dai, *J. Am. Chem. Soc.*, 2021, **143**, 8521–8526.
- 18 A. Davydov, *Molecular Spectroscopy of Oxide Catalyst Surfaces-Wiley*, John Wiley & Sons, Ltd, 2003.
- 19 Y. Sivan, J. Baraban, I. W. Un and Y. Dubi, *Science*, 2019, **364**, eaaw9367.
- 20 G. Baffou, I. Bordacchini, A. Baldi and R. Quidant, *Light:Sci. Appl.*, 2020, **9**, 108.
- 21 B. Stuart, *Infrared spectroscopy : fundamentals and applications*, J. Wiley, 2004.
- 22 M. Monai, *ACS Catal.*, 2025, **15**, 1363–1386.
- 23 J. J. Turner, M. W. George, M. Poliakoff and R. N. Perutz, *Chem. Soc. Rev.*, 2022, **51**, 5300–5329.
- 24 A. Beck, M. Gordon and P. Christopher, *J. Am. Chem. Soc.*, 2026, **148**, 7024–7034.
- 25 I. Barraza Alvarez, T. Le, H. Hosseini, S. Samira, A. Beck, J. Marlowe, M. M. Montemore, B. Wang and P. Christopher, *J. Am. Chem. Soc.*, 2024, **146**, 12431–12443.
- 26 W. F. Chen, P. Koshy and C. C. Sorrell, *Int. J. Hydrogen Energy*, 2015, **40**, 16215–16229.
- 27 V. Singh and D. T. Major, *Inorg. Chem.*, 2016, **55**, 3307–3315.
- 28 W. Shi, F. Guo, H. Wang, S. Guo, H. Li, Y. Zhou, C. Zhu, Y. Liu, H. Huang, B. Mao, Y. Liu and Z. Kang, *ACS Appl. Mater. Interfaces*, 2017, **9**, 20585–20593.
- 29 X. Li, C. Garlisi, Q. Guan, S. Anwer, K. Al-Ali, G. Palmisano and L. Zheng, *Mater. Today*, 2021, **47**, 75–107.

